# Printed-Circuit Antennas for 3-30 GHz and 3-60 GHz UWB Applications

Marjan Mokhtaari and Jens Bornemann

*Department of Electrical and Computer Engineering*
*University of Victoria, Victoria, BC, Canada*
Marjan@uvic.ca

***Abstract* — New ultra-wideband (UWB) antenna designs in printed-circuit technologies are introduced. Compared to regular UWB antennas, their frequency range is extended to cover not only the 3-10 GHz range but also the 22-29 GHz band. Altogether three designs are presented: A microstrip and a coplanar antenna operating between 3 and 30 GHz, and a coplanar design that extends the bandwidth to 60 GHz and is verified by CST and HFSS. Antenna dimensions, characteristics and performances are presented for possible applications in UWB communications systems, vehicular and other radars, through-wall imaging systems and future wireless services.**

***Index Terms* — Ultra-wideband antennas, microstrip antennas, coplanar antennas, millimeter-wave antennas.**

## I. Introduction

Since the evolution of high speed wireless networks and satellite communications and the release of ultra-wideband (UWB) frequency bands, UWB components have found increasing applications [1]. The ultra-wideband antenna is an essential front-end component, and different configurations and technologies are used in applications ranging from radio astronomy, e.g. [2], over EMC compliance, e.g. [3], to medical monitoring, e.g. [4]. Printed-circuit realization of UWB antennas, especially in microstrip and coplanar circuitry, e.g. [5], is attractive due to low-cost fabrication, high design flexibility, small size and low weight.

However, the vast majority of printed-circuit UWB antenna designs focus on the 3-10 GHz region. Only rarely is a structure designed to cover higher frequencies such as the 6-40 GHz band in [6] with potential applications in the vehicular radar band (22-29 GHz) or through-wall imaging systems [7].

Therefore, this paper focuses on the design of UWB antennas that extend the 3-10 GHz range all the way up to 30 GHz and 60 GHz to provide designs that are simultaneously applicable to a variety of UWB services such as wireless communication, vehicular radars, through-wall imaging systems and a wide range of future applications.

## II. Antenna Designs and Results

Since synthesis methods of printed-circuit UWB antennas do not exist, the configurations in this paper are obtained by modifying previous designs, especially that of the stepped coplanar antenna in [8]. Analyses and fine optimizations are performed in a CST Microwave Studio environment which has previously compared well to HFSS and measurements in the 3-10 GHz [4] and the 6-40 GHz ranges [6]. As an initial investigation, the input return loss bandwidth of a UWB microstrip antenna was calculated for varying substrates and substrate thickness. While thicker substrates can be allowed in the traditional 3-10 GHz UWB range, lower permittivities and substrate heights are required for operation into millimeter-wave bands.

### *A. 3-30 GHz Antennas*

Therefore, the first two antennas are designed on RT 6002 with $\varepsilon_r$=2.94 and height $h$=762μm (30 mils). Fig. 1 shows the outlines and dimensions of a microstrip (Fig. 1a) and coplanar antenna (Fig. 1b).

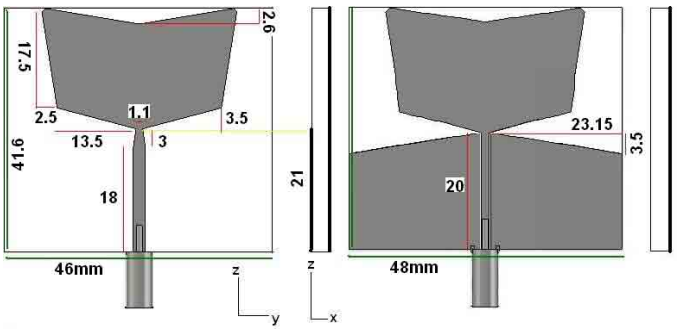


(a) (b)

Fig. 1. Schematic views of 3-30 GHz UWB antennas in microstrip (a) and coplanar (b) technologies (dimensions in mm).

The reflection coefficients of both antennas are shown in Fig. 2 and cover a 10dB bandwidth from 2.2 GHz to more than 30 GHz. Note that the EM simulations of the entire structures include input coaxial feed lines with K connectors which are also used in the coplanar design to connect the left and right ground planes.

Fig. 3 depicts co- and cross-polarization performances with a probe positioned in the far field at $\theta$=90° and $\phi$=90°. (Angles are taken as per convention with $\theta$ down from the vertical $z$ direction and $\phi$ from the $x$ to the $y$ axis.) The polarization is predominantly vertical in the lower frequency range, but cross-polar components increase with frequency and thus give rise to dual-polarization applications for frequencies above 22 GHz. Note that the cross-polar component of the microstrip antenna is, in general, higher

 

than that of the coplanar one. This is due to the field rotation from the *x* direction in the microstrip feed to the co-polarized *yz* field while the coplanar feed field is already in the *yz* plane.

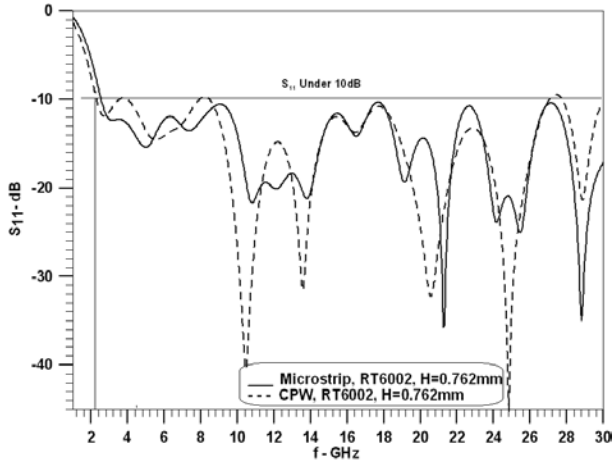


Fig. 2. Input reflection coefficient performances of microstrip and coplanar (CPW) antennas in Fig. 1.

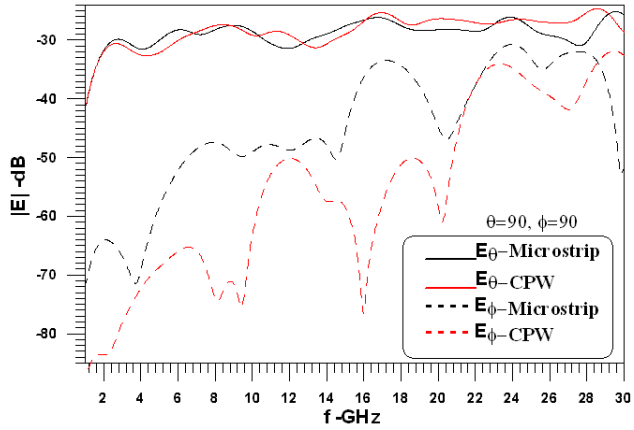


Fig. 3. Amplitude responses of co- and cross-polarized electric fields for microstrip and coplanar (CPW) antennas in Fig. 1 with probes located at $\theta=90^o$ and $\phi=90^o$.

Radiation patterns have been calculated but cannot be displayed here for lack of space. The E-plane patterns resemble that of a dipole with some variation in the angular dependence as the frequency increases from 3 GHz all the way to 30 GHz. The H-plane patterns are omnidirectional in principle with minima appearing (in the high frequency range) at $\pm60^o$ of $\phi=0^o$ and $\phi=180^o$. However, for the entire frequency range, the field is maximum at $\theta=90^o$ and $\phi=\pm90^o$ as expected from a vertical dipole.

Many gain plots of UWB antennas show the maximum gain versus frequency. This is misleading, however, since the direction, in which the maximum gain is achieved, changes with frequency, and the direction of maximum gain versus frequency is usually not shown. Therefore, we present in Fig. 4 the gains of the two antennas in Fig. 1 in the preferred direction of $\theta=90^o$ and $\phi=90^o$. It is observed that above 16 GHz, the gain of the coplanar UWB antenna is approximately 2 dB higher that that of the microstrip antenna. In the lower frequency range, between 3GHz and 14 GHz, the gain in the given direction drops below 0 dB at certain frequencies. Since the gain computation is subject to integration over a sphere, negative gain indicates that the direction of maximum gain is not close to $\theta=90^o$ and $\phi=90^o$. The relatively small variation of E-field levels at those frequencies in Fig. 3 is consistent with this interpretation.

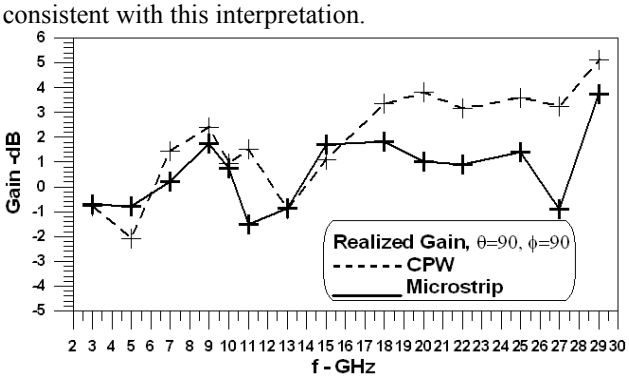


Fig. 4. Realized gain performances for microstrip and coplanar (CPW) antennas in Fig. 1 with probes located at $\theta=90^o$ and $\phi=90^o$.

An essential parameter evaluated in UWB antenna designs for wireless communications is group delay. It is determined from the transfer function between the antenna's input (the coaxial connectors in Fig. 1) and a probe in the far field of the antenna. The probes have been placed at two locations - $\theta=90^o$, $\phi=90^o$ and $\theta=90^o$, $\phi=0^o$. Fig. 5 shows the group delay responses of vertical and horizontal polarization at the two distinctive far field probes' locations. The group delay variations for the co-polarized fields in $\theta=90^o$, $\phi=90^o$ direction are 180 ps for the microstrip antenna (Fig. 5a) and 150 ps for the coplanar antenna (Fig. 5b). These values are comparable with results reported in the literature, but it is noted that the ones presented here hold up to 30 GHz. Several peaks appear for horizontal polarization (cross polarization) in Fig. 5a and Fig. 5b. For the second probe at $\theta=90^o$, $\phi=0^o$, the only group-delay level acceptable in Fig. 5c and Fig. 5d is that of the horizontal polarization of the microstrip antenna (dashed line in Fig. 5c). In connection with the data presented in Fig. 3, Fig. 5a and Fig. 5c, this indicates possible dual-polarized application of the microstrip antenna in the 22 - 30 GHz frequency range.

*B. 3-60 GHz Antenna*

In order to further increase the bandwidth of printed-circuit UWB antennas, designs must use lower-permittivity substrate material with smaller thickness. Fig. 6 shows the layout and dimensions of a coplanar UWB antenna on RT 5870 with $\varepsilon_r=2.35$ and height $h=254\mu m$ (10 mils). Similarly, the frequency range of the coaxial cable feeding the antenna is changed to reflect those of V connectors.

The input reflection performance is depicted in Fig. 7 and confirms operation between 3.2 GHz and 60 GHz. Excellent agreement is observed between the time-domain computations in CST and the frequency-domain HFSS results up to 50 GHz. Above 50 GHz, the results deviate slightly

since the highest meshing frequency in HFSS was set to 50 GHz to obtain results within a reasonable time frame.

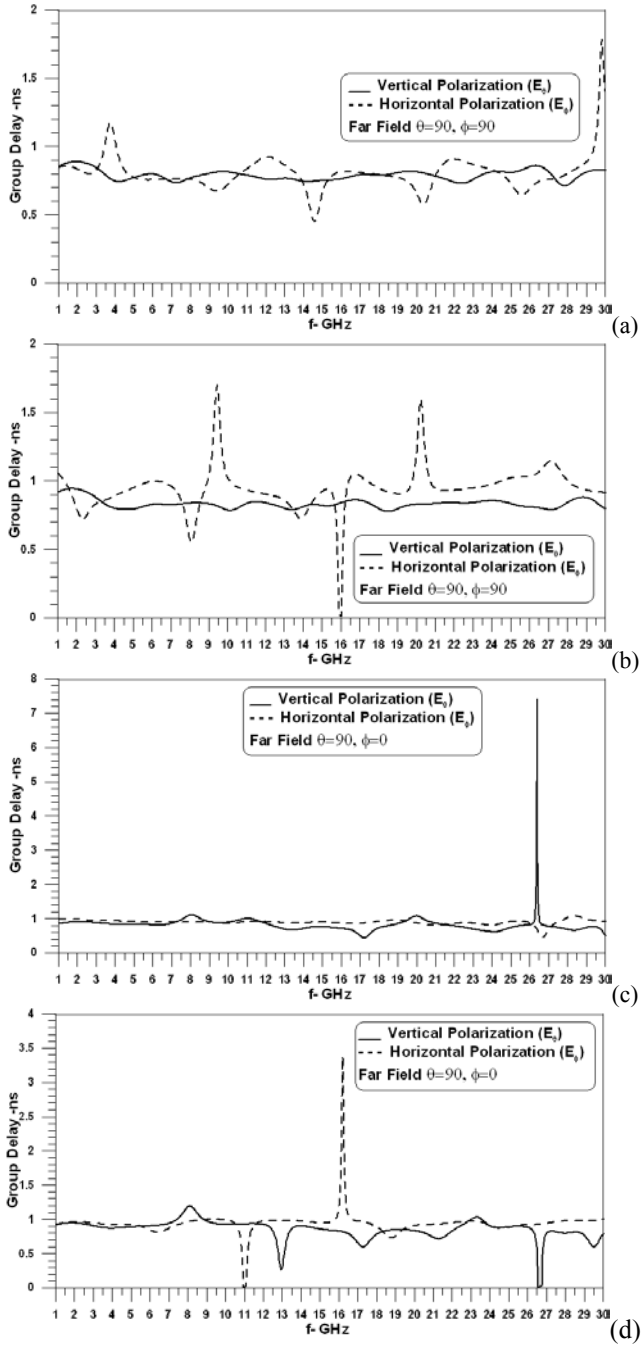


Fig. 5. Group delay responses for both vertical ($E_\theta$) and horizontal ($E_\phi$) polarizations for microstrip (a,c) and coplanar (b,d) antennas in Fig. 1 with probes located at $\theta=90^o$, $\phi=90^o$ and $\theta=90^o$, $\phi=0^o$.

Fig. 8 shows the received co- and cross polarized fields for a probe located at of $\theta=90^o$ and $\phi=90^o$. The co-polarized field is more than 10 dB above the cross-polarized one and thus determines the linear vertical polarization of this UWB antenna.

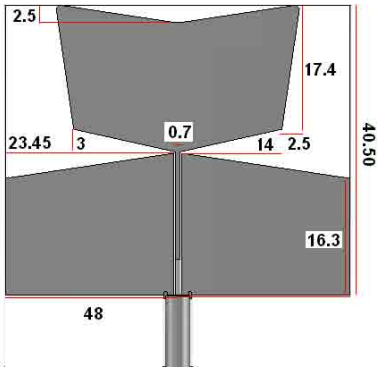


Fig. 6. Schematic front view of the 3-60 GHz UWB antenna in coplanar technology on RT5870 material and thickness of 254μm (10 mils). (All dimensions in mm.)

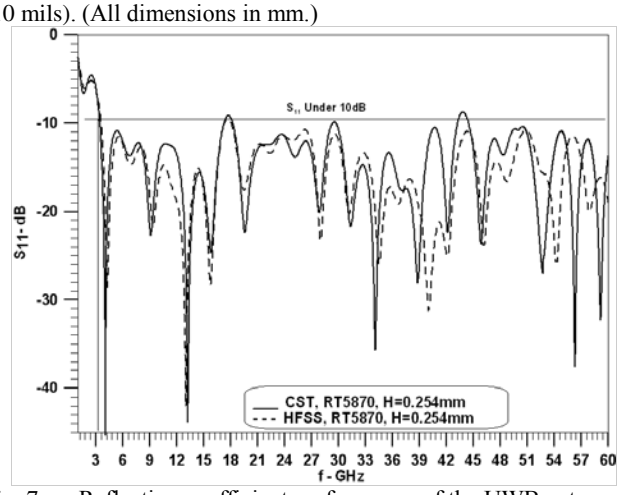


Fig. 7. Reflection coefficient performance of the UWB antenna in Fig. 6; comparison between CST Microwave Studio (time domain) and HFSS (frequency domain).

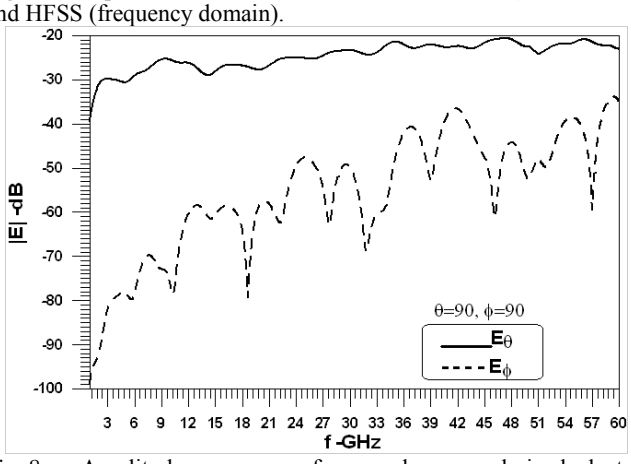


Fig. 8. Amplitude responses of co- and cross-polarized electric fields for the coplanar (CPW) antenna in Fig. 6 with probes located at $\theta=90^o$ and $\phi=90^o$.

Fig. 9 depicts the gain performance of the UWB antenna in Fig. 6. The three curves can be viewed as follows: The realized gain is the gain in the direction of $\theta=90^o$, $\phi=90^o$. This gain is below 0 dB in the lower frequency range as the direction of maximum gain changes with frequency. The E-plane plot in Fig. 9 is the maximum gain obtained at varying angles θ in the E-plane, i.e., the *yz* plane in Fig. 1. The H-plane gain is the maximum gain at varying angles ϕ in the H-

plane. It is observed that for f ≥ 9 GHz, the maximum H-plane gain is actually in the direction of of θ=90°, ϕ=90° as these two curves match in Fig. 9. Above 27 GHz, the three gain curves start to align, thus confirming the above direction as the main beam.

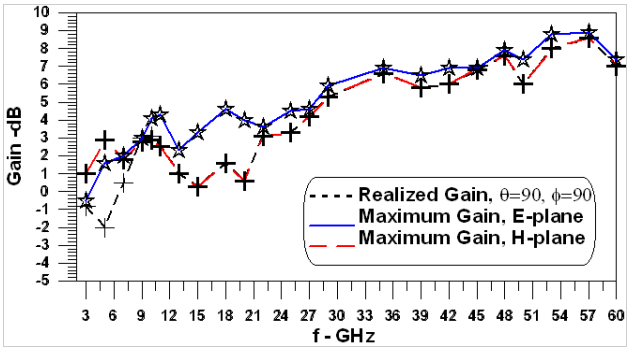


Fig. 9. Gain power performances of UWB antenna in Fig. 6; gain in θ=90°, ϕ=90° direction and maximum gains in E- and H-plane (varying directions).

Finally, Fig. 10 demonstrates the group delay performance of the two polarizations, again with probes in the direction of of θ=90°, ϕ=90°. The group delay variation for the vertical polarization (co-pol) is less than 150ps up to 60 GHz, which is comparable to other printed-circuit UWB antennas over only the 3-10 GHz range.

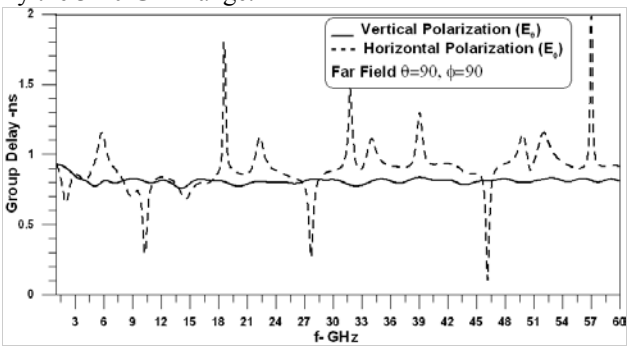


Fig. 10. Group delay performance of vertical and horizontal polarization of UWB antenna in Fig. 6 with probes located at θ=90° and ϕ=90°.

## III. Conclusions

Three different printed-circuit UWB antennas are presented that extend the 3-10 GHz range to include the 22-29 GHz region and even go up to 60 GHz.

A comparison between 3-30 GHz microstrip and coplanar antennas reveals that the coplanar antenna performs better in co-polarized operation. However, the microstrip antenna shows possibilities for dual-polarization applications in the 22-29 GHz range while maintaining linear polarization between 3 GHz and 14 GHz.

As substrate material and thickness influences the highest frequency of operation, a coplanar antenna is designed on a different substrate up to 60 GHz. For this coplanar antenna, co- to-cross-polar isolation is observed to be better than 10 dB over the entire 3-60 GHz band, and the maximum group-delay variation for the same frequency range is 150 ps.

The designs demonstrate that bandwidths in extend of a decade frequencies are possible with simple printed-circuit antennas.

## Acknowledgement

The authors wish to acknowledge support for this work from the Natural Sciences and Engineering Research Council of Canada and the TELUS Research Grant in Wireless Communications.

## References

[1] L. Yang and G.B. Giannakis, "Ultra-wideband communications: An idea whose time has come," *IEEE Signal Proc. Mag.*, Vol. 21, pp.26-54, Nov. 2004

[2] P.-S. Kildal, R. Olsson and J. Yang, "Development of three models of the Eleven antenna: A new decade bandwidth high performance feed for reectors," Proc. European Conf. Antennas Propagat., pp. 1-6, Nov. 2006.

[3] J.D. Brunett, R.M. Ringler and V.V. Liepa, "On measurements for EIRP compliance of UWB devices," *IEEE EMC-S Int. EMC Symp. Dig.*, Vol. 2. pp. 473-476, Aug. 2005

[4] H.-J. Lam and J. Bornemann, "Ultra-wideband printed-circuit array antenna for medical monitoring applications", *Proc. 2009 IEEE Int. Conf. Ultra-Wideband*, pp. 506-510, Sep. 2009.

[5] H.-J. Lam, Y. Lu, H. Du, P.P.M. So and J. Bornemann, "Time-domain modelling of group-delay and amplitude characteristics in ultra-wideband printed-circuit antennas", pp. 321-331 in *Springer Proceedings in Physics 121*, (P. Russer, U. Siart eds.), Springer, Berlin 2008.

[6] K. Rambabu, H.A. Thiart, J. Bornemann and S.Y. Yu, "Ultrawideband printed-circuit antenna", *IEEE Trans. Antennas Propagat.*, Vol. 54, pp. 3908-3911, Dec. 2006.

[7] Federal Communications Commission (FCC), Revision of Part 15 of the Commission's Rules Regarding Ultra-Wideband Transmission Systems, First Report and Order, FCC 02-48, 2002.

[8] H.-J. Lam and J. Bornemann, "Ultra-wideband printed-circuit antenna in coplanar technology", in *2007 IEEE EMC-S Int. Symp. Dig.*, TU-PM-1-7, 4 p., July 2007.